fitness maximum, suggesting that the broader topography of adaptive landscapes is more strongly determined by stable performance constraints than frequency-dependent dynamics.

References and Notes

1. D. Schluter, *The Ecology of Adaptive Radiation* (Oxford Univ. Press, Cambridge, 2000).
2. G. G. Simpson, *Tempo and Mode in Evolution* (Columbia Univ. Press, New York, 1944).
3. R. Lande, *Evolution* **33**, 402 (1979).
4. E. I. Svensson, R. Calsbeek, *The Adaptive Landscape in Evolutionary Biology* (Oxford Univ. Press, Oxford, 2012).
5. S. Wright, *Proc. VI Int. Cong. Gen.* **1**, 356 (1932).
6. M. Foote, *Annu. Rev. Ecol. Syst.* **28**, 129 (1997).
7. D. L. Rabosky, I. J. Lovette, *Proc. Biol. Sci.* **275**, 2363 (2008).
8. L. J. Harmon *et al.*, *Evolution* **64**, 2385 (2010).
9. J. G. Kingsolver *et al.*, *Am. Nat.* **157**, 245 (2001).
10. C. H. Martin, *Am. Nat.* **180**, E90 (2012).
11. A. P. Hendry, S. K. Huber, L. F. De León, A. Herrel, J. Podos, *Proc. Biol. Sci.* **276**, 753 (2009).
12. D. Schluter, *Science* **266**, 798 (1994).
13. C. W. Benkman, *Evolution* **57**, 1176 (2003).
14. R. Calsbeek, D. J. Irschick, *Evolution* **61**, 2493 (2007).
15. C. S. McBride, M. C. Singer, *PLoS Biol.* **8**, e1000529 (2010).
16. E. Svensson, B. Sinervo, *Evolution* **54**, 1396 (2000).
17. D. W. Schemske, H. D. Bradshaw Jr., *Proc. Natl. Acad. Sci. U.S.A.* **96**, 11910 (1999).
18. D. Schluter, P. R. Grant, *Am. Nat.* **123**, 175 (1984).
19. C. H. Martin, P. C. Wainwright, *Evolution* **65**, 2197 (2011).
20. Additional supporting data and analyses are available in the supplementary materials on *Science* Online.

Acknowledgments: Funded by NSF grant DDIG DEB-1010849, the Gerace Research Centre, and the Center for Population Biology. Permits were approved by the Bahamian government and the University of California, Davis. G. Mount and S. Romero assisted with research; T. Schoener, M. Turelli, A. Hendry, D. Nychka, L. Schmitz, and C. Boettiger provided feedback. C.H.M. designed the study, raised funding, performed research, collected and analyzed data, and wrote the paper. P.C.W. contributed materials, discussed design and results, and commented on the manuscript.

Supplementary Materials

www.sciencemag.org/cgi/content/full/339/6116/208/DC1
Materials and Methods
Figs. S1 to S9
Tables S1 to S9
References (*21*–*51*)

20 July 2012; accepted 16 November 2012
10.1126/science.1227710

Suppression of Oxidative Stress by β-Hydroxybutyrate, an Endogenous Histone Deacetylase Inhibitor

Tadahiro Shimazu,[1,2] Matthew D. Hirschey,[1,2] John Newman,[1,2] Wenjuan He,[1,2] Kotaro Shirakawa,[1,2] Natacha Le Moan,[3] Carrie A. Grueter,[4,5] Hyungwook Lim,[1,2] Laura R. Saunders,[1,2] Robert D. Stevens,[6] Christopher B. Newgard,[6] Robert V. Farese Jr.,[2,4,5] Rafael de Cabo,[7] Scott Ulrich,[8] Katerina Akassoglou,[3] Eric Verdin[1,2]*

Concentrations of acetyl–coenzyme A and nicotinamide adenine dinucleotide (NAD^+) affect histone acetylation and thereby couple cellular metabolic status and transcriptional regulation. We report that the ketone body D-β-hydroxybutyrate (βOHB) is an endogenous and specific inhibitor of class I histone deacetylases (HDACs). Administration of exogenous βOHB, or fasting or calorie restriction, two conditions associated with increased βOHB abundance, all increased global histone acetylation in mouse tissues. Inhibition of HDAC by βOHB was correlated with global changes in transcription, including that of the genes encoding oxidative stress resistance factors FOXO3A and MT2. Treatment of cells with βOHB increased histone acetylation at the *Foxo3a* and *Mt2* promoters, and both genes were activated by selective depletion of HDAC1 and HDAC2. Consistent with increased FOXO3A and MT2 activity, treatment of mice with βOHB conferred substantial protection against oxidative stress.

Cellular metabolites such as acetyl–coenzyme A (acetyl-CoA) and nicotinamide adenine dinucleotide (NAD^+) influence gene expression by serving as cofactors for epigenetic modifiers that mediate posttranslational modification of histones (*1*). The activity of histone acetyltransferases (HATs) is dependent on nuclear acetyl-CoA concentrations (*2*, *3*) and the deacetylase activity of class III HDACs, also called sirtuins, is dependent on NAD^+ concentrations (*4*). Class I (HDAC1, 2, 3, 8), class II (HDAC4, 5, 6, 7, 9, 10), and class IV (HDAC11) HDACs are zinc-dependent enzymes, but endogenous regulators are not known.

Small-molecule inhibitors of class I and class II HDACs include butyrate, a product of bacterial anaerobic fermentation (*5*). Butyrate is closely related to β-hydroxybutyrate (βOHB) (Fig. 1A), the major source of energy for mammals during prolonged exercise or starvation (*6*). Accumulation of βOHB in blood increases to 1 to 2 mM during fasting when the liver switches to fatty acid oxidation (*7*, *8*), and to even higher concentrations during prolonged fasting (6 to 8 mM) (*6*) or in diabetic ketoacidosis (>25 mM) (*9*).

To determine whether βOHB might have HDAC inhibitor activity, we treated human embryonic kidney 293 (HEK293) cells with different amounts of βOHB for 8 hours, and measured histone acetylation levels by Western blot with antibodies to acetylated histone H3 lysine 9 ($AcH3_{K9}$) and to acetylated histone H3 lysine 14 ($AcH3_{K14}$) (Fig. 1, B and C, and figs. S1 and S2). βOHB increased histone acetylation in a dose-dependent manner, even at 1 to 2 mM, which can occur in humans after a 2- to 3-day fast or strenuous exercise (*6*, *8*, *10*). Like butyrate, βOHB did not increase acetylation of α-tubulin, indicating that it inhibits class I HDACs but not the class IIb tubulin deacetylase, HDAC6.

To test the HDAC inhibitor activity of βOHB and its possible selectivity, we purified recombinant human HDACs after transient transfection of expression vectors for human epitope-tagged (FLAG) HDAC1, HDAC3, HDAC4, and HDAC6 in HEK293T cells. We purified the HDACs, incubated them with ^3H-labeled acetylated histone H4 peptides, and measured their deacetylase activity (Fig. 1D) (*11*). βOHB inhibited HDAC1, HDAC3, and HDAC4 in a dose-dependent manner with a median inhibitory concentration (IC_{50}) of 5.3, 2.4, and 4.5 mM, respectively. The HDAC6 IC_{50} was much higher (48.5 mM) (Fig. 1E), and βOHB did not inhibit HDAC6 activity on its natural substrate tubulin (fig. S3). To examine the possibility that histone acetylation was enhanced by increased concentration of acetyl-CoA (because βOHB is catabolized into acetyl-CoA in target tissues), we directly measured abundance of acetyl-CoA in βOHB-treated HEK293 cells, but no change was observed (fig. S4). We also tested a possible activating effect of βOHB on histone acetyltransferase activity of p300 and PCAF (P300/CBP-associated factor) but did not detect any change induced by βOHB (fig. S5). Thus, millimolar concentrations of βOHB appear to increase histone acetylation directly through HDAC inhibition. High concentrations of acetoacetate (AcAc) also inhibit class I and class IIa HDACs in vitro (fig. S6A) and in HEK293 cells (fig. S6B). However, the concentration of AcAc in blood is one-third or less than that of βOHB during fasting and therefore less likely to reach concentrations that would inhibit HDACs under physiological conditions (*12*). To test the relative contribution of βOHB,

[1]Gladstone Institute of Virology and Immunology, San Francisco, CA 94158, USA. [2]Department of Medicine, University of California, San Francisco, CA 94143, USA. [3]Gladstone Institute of Neurological Disease, San Francisco, CA 94158, USA. [4]Gladstone Institute of Cardiovascular Disease, San Francisco, CA 94158, USA. [5]Department of Biochemistry and Biophysics, University of California, San Francisco, CA 94143, USA. [6]Sarah W. Stedman Nutrition and Metabolism Center, and Departments of Pharmacology and Cancer Biology and Medicine, Duke University Medical Center, Durham, NC 27704, USA. [7]Laboratory of Experimental Gerontology, National Institute on Aging, National Institutes of Health, Baltimore, MD 21224, USA. [8]Department of Chemistry, Ithaca College, Ithaca, NY 14850, USA.

*To whom correspondence should be addressed. E-mail: everdin@gladstone.ucsf.edu

acetoacetate, and acetyl-CoA to histone acetylation in response to βOHB treatment, we depleted cells of βOHB dehydrogenases (BDH1, 2) with small interfering RNA. Both enzymes catalyze the transformation of βOHB into acetoacetate, and their suppression had no effect on histone acetylation in response to βOHB up to 3mM. At higher concentrations of βOHB (10 and 30 mM), however, further increase in histone acetylation was suppressed by depletion of βOHB dehydrogenases (fig. S7, A and B), indicating that either AcAc or acetyl-CoA might also contribute to histone acetylation in cells exposed to concentrations of βOHB above the IC_{50} for HDACs.

To determine whether changes in βOHB concentrations in vivo might affect histone acetylation, we measured βOHB concentration in mouse serum after a 24-hour fast or in mice on calorie restriction (CR). We also used implanted osmotic pumps to administer exogenous βOHB or phosphate-buffered saline (PBS). βOHB concentrations increased to 1.5 ± 0.1 mM after a 24-hour fast, 0.6 ± 0.1 mM in mice on CR and 1.2 ± 0.1 mM with administration of βOHB via an intraperitoneal pump (Fig. 2A). We collected tissues from fed or 24-hour–fasted mice and measured histone acetylation by immunoblotting. Acetylation of $H3_{K9}$ and $H3_{K14}$ reflect the competing activities of HATs and HDACs and influence gene expression in several species, including humans (*13*). Acetylation of $H3_{K9}$ and $H3_{K14}$ increased significantly in several organs in fasted mice, particularly kidney (Fig. 2B and figs. S8 and S9). In kidney, histone acetylation ($H3_{K9}$ and $H3_{K14}$) also increased two- to fivefold in mice under CR. Kidney histone acetylation and serum βOHB concentrations were strongly correlated for both histone $H3_{K9}$ (R^2 = 0.772) and histone $H3_{K14}$ (R^2 = 0.863) (Fig. 2C). We first focused on kidney, the organ with the largest changes in histone acetylation, to investigate the effects

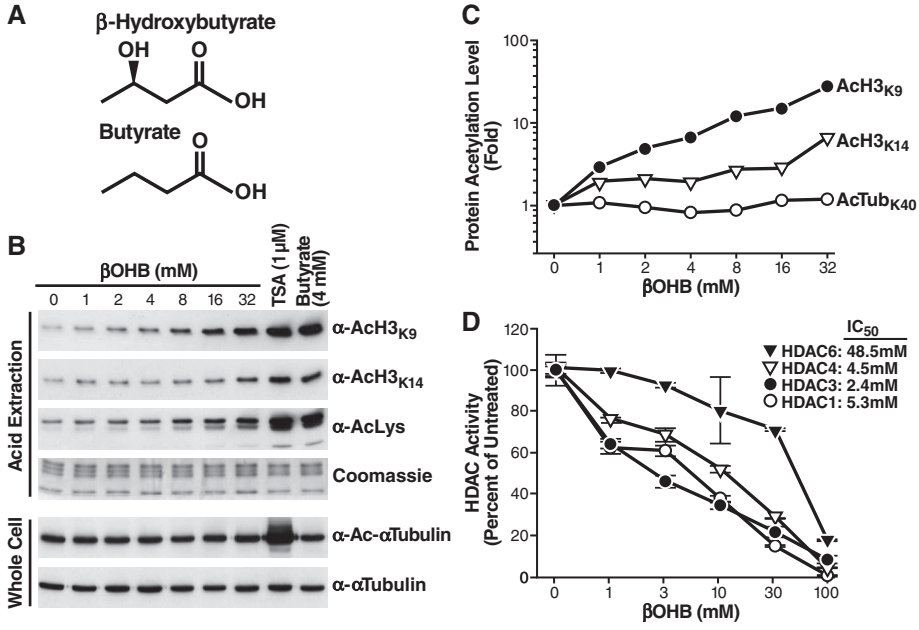

Fig. 1. Inhibition of HDACs by βOHB in vitro and in vivo. (**A**) Structures of β-hydroxybutyrate and butyrate. (**B**) Effect of βOHB, TSA, or butyrate on acetylation of histone H3 and tubulin. HEK293 cells were treated with the indicated concentrations of drugs for 8 hours. Histones were acid-extracted, and their acetylation was assessed by protein immunoblotting with anti-$AcH3_{K9}$, anti-$AcH3_{K14}$, or anti-acetyllysine (AcLys). Proteins from whole-cell extracts were analyzed by immunoblotting with antibodies to α-tubulin or Ac-α-Tubulin. (**C**) Quantification of acetylation levels from blots in (B), shown relative to untreated cells (βOHB 0 mM). (**D**) Inhibition of immunopurified HDACs by βOHB in vitro. Flag-tagged HDACs were expressed in HEK293 cells, immunoprecipitated, and incubated in vitro with a ^{3}H-labeled acetylated histone H4 peptide and the indicated concentrations of βOHB. HDAC activity is relative to the activity of each enzyme without βOHB. The IC_{50} values of βOHB are shown.

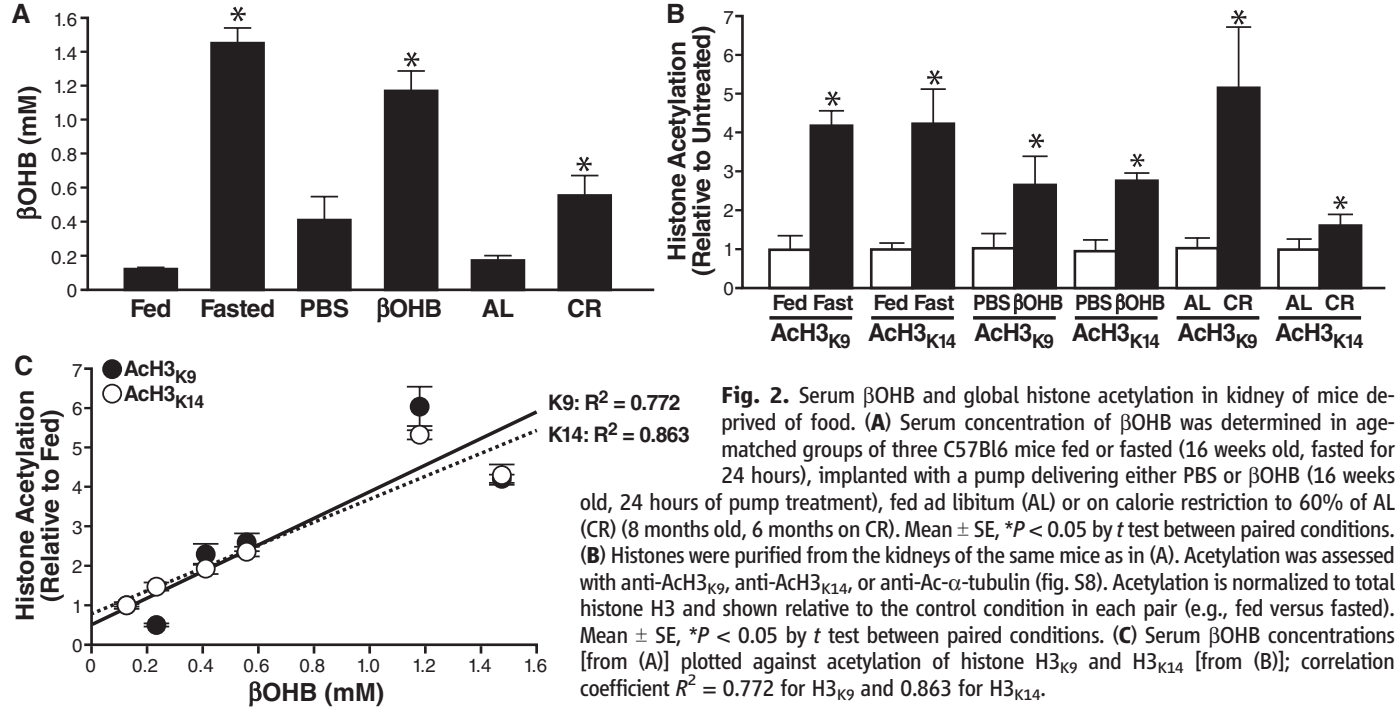

Fig. 2. Serum βOHB and global histone acetylation in kidney of mice deprived of food. (**A**) Serum concentration of βOHB was determined in age-matched groups of three C57Bl6 mice fed or fasted (16 weeks old, fasted for 24 hours), implanted with a pump delivering either PBS or βOHB (16 weeks old, 24 hours of pump treatment), fed ad libitum (AL) or on calorie restriction to 60% of AL (CR) (8 months old, 6 months on CR). Mean ± SE, *$P < 0.05$ by *t* test between paired conditions. (**B**) Histones were purified from the kidneys of the same mice as in (A). Acetylation was assessed with anti-$AcH3_{K9}$, anti-$AcH3_{K14}$, or anti-Ac-α-tubulin (fig. S8). Acetylation is normalized to total histone H3 and shown relative to the control condition in each pair (e.g., fed versus fasted). Mean ± SE, *$P < 0.05$ by *t* test between paired conditions. (**C**) Serum βOHB concentrations [from (A)] plotted against acetylation of histone $H3_{K9}$ and $H3_{K14}$ [from (B)]; correlation coefficient R^2 = 0.772 for $H3_{K9}$ and 0.863 for $H3_{K14}$.

of βOHB on gene expression and cellular phenotype.

Histone acetylation induced by HDAC inhibitors is associated with transcriptional activation and repression of a subset of cellular genes (*14*). To identify genes whose expression changed in response to βOHB, we extracted mRNA for microarray analysis from mouse kidneys treated with βOHB or PBS for 24 hours. As βOHB is more abundant in fasting conditions, gene expression changes induced by βOHB may be a subset of those induced by fasting. Of 35,556 genes tested, 284 increased transcription in response to fasting (false discovery rate <0.2, table S1). Four of the five genes with the largest changes in expression in response to βOHB were also activated in response to fasting as determined both by microarray and quantitative real-time polymerase chain reaction (QPCR) ($P < 0.001$ for such overlap via binomial distribution, tables S2 and S3). Ingenuity pathway analysis identified two of the five βOHB-induced genes (*Mt2* and *Lcn2*) as regulated by FOXO3A. Overall, we found five genes in the FOXO3A network (*Foxo3a*, *Mt2*, *Lcn2*, *Lemd3*, and *Hbp1*) that had increased transcription in response to βOHB via QPCR (fig. S10). *Foxo3a*, a transcription factor, induces cell-cycle arrest and resistance to oxidative stress (*15*). Metallothionein 2 (*Mt2*), the gene with the greatest transcriptional response to βOHB treatment as determined by QPCR, also protects against oxidative stress (*16*). *Foxo3a* and *Mt2* mRNA expression is also modestly increased during CR as determined by QPCR (Fig. 3, A and B). Chromatin immunoprecipitation (ChIP) analysis of the *Foxo3a* and *Mt2* promoters with two distinct primer pairs for each promoter revealed increased histone $H3_{K9}$ acetylation at both promoters after treatment of HEK293 cells with a high dose of βOHB (10 mM) (Fig. 3C).

Next, we depleted cells of each class I and II HDAC with selective short hairpin–mediated RNAs (shRNAs). The shRNAs selective for each HDAC suppressed expression of their cognate HDAC by at least 60% (fig. S11). Depletion of HDAC1 or HDAC2 caused up-regulation of *Foxo3a* and *Mt2* mRNA by 1.8-fold and 1.5-fold, respectively (Fig. 3D). Depletion of both HDAC1 and 2 further increased accumulation of *Foxo3a* and *Mt2* mRNA (Fig. 3D). ChIP analysis revealed that HDAC1, but not HDAC6, was recruited to the *Foxo3a* and *Mt2* promoters and not recruited to the *Gapdh* promoter (Fig. 3E). Binding of HDAC1 to the *Foxo3a* promoter was unchanged by βOHB treatment; thus, HDAC catalytic activity appears not to be necessary for promoter binding of HDAC1 (fig. S12). βOHB appears to induce local histone acetylation at the promoter of oxidative stress resistance genes, *Foxo3a* and *Mt2*, by inhibiting activity of HDACs 1 and 2.

Mitochondrial superoxide dismutase (Mn-SOD) and catalase are two other well-defined FOXO3A targets that contribute to its protective activity against oxidative stress (*15*, *17*). Protein immunoblotting of kidney tissue isolated from PBS- or βOHB-treated mice showed increased expression of FOXO3A, Mn-SOD, and catalase (Fig. 4A and figs. S13 and S14) .

The effect on expression of MT2, FOXO3A, MnSOD, and catalase indicated that βOHB might have protective activity against oxidative stress. Carbonyl derivatives are formed by a direct metal-catalyzed oxidative attack on the amino acid side chains of proline, arginine, lysine, and threonine. Carbonylation is irreversible and unrepairable and accumulates as organisms age (*18*). To test the possible protective role of βOHB against oxidative stress, we implanted mice with a subcutaneous pump delivering either βOHB or PBS for 24 hours. They then received an intravenous injection of paraquat, which induces accumulation of reactive oxygen species. Kidney tissue was isolated after

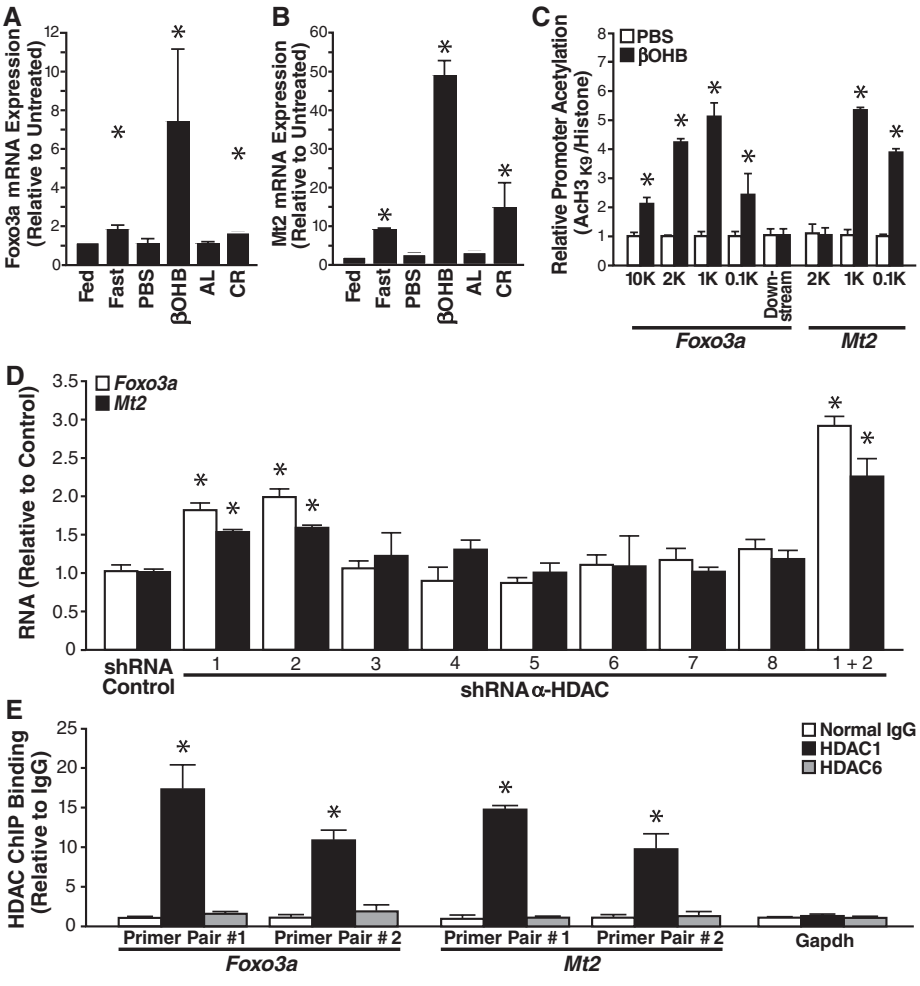

Fig. 3. Increased expression of oxidative stress resistance genes in cells exposed to βOHB. (**A**) Expression of *Foxo3a* under various conditions (see Fig. 2 for details) measured by QPCR. *Foxo3* expression is normalized to abundance of glyceraldehyde-3-phosphate dehydrogenase (GAPDH). Mean ± SE, *$P < 0.05$ by *t* test between paired conditions. (**B**) Expression of *Mt2*, measured as in (A). (**C**) Promoters of *Mt2* and *Foxo3a* are enriched for acetylated histone H3K9 after βOHB treatment. HEK293 cells were treated with 10 mM βOHB or PBS for 24 hours. Chromatin was immunoprecipitated with anti-H3 or anti-$AcH3_{K9}$, and the purified DNA was analyzed with primer pairs specific for the *Foxo3a* or *Mt2* promoters. Results are the ratios of $AcH3_{K9}$ to total histone H3. Mean ± SE, *$P < 0.05$ by *t* test between βOHB and PBS conditions. (**D**) HDAC depletion increases *Foxo3a* and *Mt2* mRNAs abundance. HEK293 cells were transfected with shRNAs specific for each class I or class II HDAC, and mRNA abundance was measured by QPCR 72 hours after transfection. Mean ± SE, *$P < 0.05$ by *t* test versus control shRNA. (**E**) HDAC1, but not HDAC6, is enriched at the promoters of *Mt2* and *Foxo3a*. ChIP analysis of the *Foxo3a* and *Mt2* promoters (two primer pairs per promoter) and Gapdh (one primer pair) from HEK293 cells with control immunoglobulin G (IgG), anti-HDAC1, or anti-HDAC6. Relative promoter binding of each HDAC is normalized to input Gapdh. Mean ± SE, *$P < 0.05$ by *t* test versus IgG control.

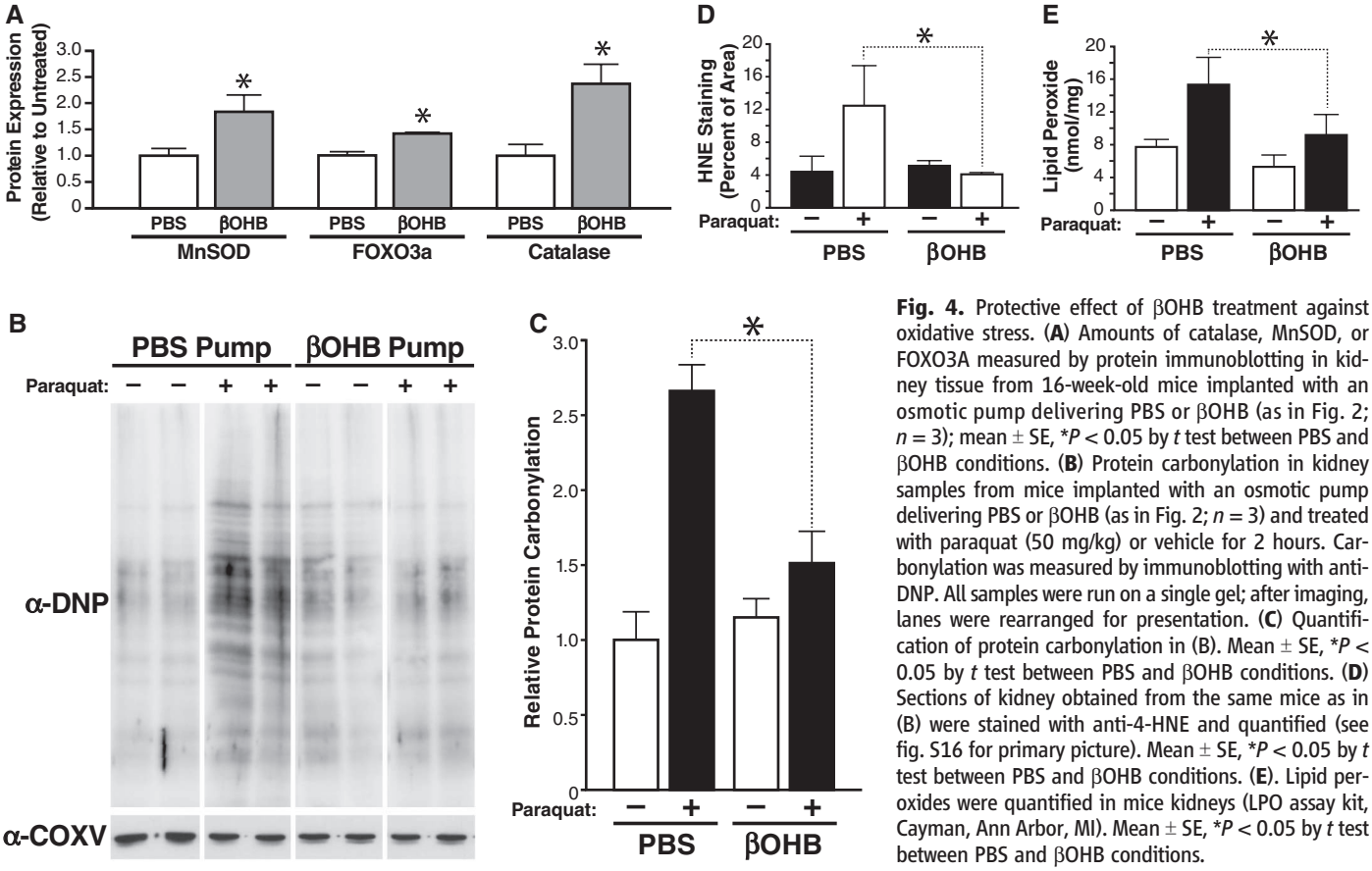

Fig. 4. Protective effect of βOHB treatment against oxidative stress. (**A**) Amounts of catalase, MnSOD, or FOXO3A measured by protein immunoblotting in kidney tissue from 16-week-old mice implanted with an osmotic pump delivering PBS or βOHB (as in Fig. 2; $n = 3$); mean ± SE, $^*P < 0.05$ by t test between PBS and βOHB conditions. (**B**) Protein carbonylation in kidney samples from mice implanted with an osmotic pump delivering PBS or βOHB (as in Fig. 2; $n = 3$) and treated with paraquat (50 mg/kg) or vehicle for 2 hours. Carbonylation was measured by immunoblotting with anti-DNP. All samples were run on a single gel; after imaging, lanes were rearranged for presentation. (**C**) Quantification of protein carbonylation in (B). Mean ± SE, $^*P < 0.05$ by t test between PBS and βOHB conditions. (**D**) Sections of kidney obtained from the same mice as in (B) were stained with anti-4-HNE and quantified (see fig. S16 for primary picture). Mean ± SE, $^*P < 0.05$ by t test between PBS and βOHB conditions. (**E**). Lipid peroxides were quantified in mice kidneys (LPO assay kit, Cayman, Ann Arbor, MI). Mean ± SE, $^*P < 0.05$ by t test between PBS and βOHB conditions.

2 hours, and protein carbonylation was assayed by protein immunoblotting with an antibody to dinitrophenyl (DNP) after derivatization of protein with dinitrophenylhydrazine (DNPH) (Fig. 4B). Paraquat treatment of control mice receiving a PBS infusion led to a twofold increase in carbonylated proteins. This increase in protein carbonylation was significantly suppressed (54 ± 9% decrease) in mice receiving βOHB (Fig. 4C).

We also examined another marker of oxidative stress: lipid peroxidation. 4-Hydroxynonenal (4-HNE) is a degradation product of polyunsaturated lipid and accumulates in response to oxidative stress (*19*). Kidney tissue sections from PBS- or paraquat-treated mice were stained with an antibody to 4-HNE, and the amount of 4-HNE staining was quantified with imaging software (fig. S15). Paraquat treatment increased 4-HNE staining threefold in control mice (PBS) (Fig. 4D). This increase was completely suppressed in mice treated with βOHB. Lipid peroxides were also directly quantified in an enzyme-linked immunosorbent assay that measures conversion of ferrous ions to ferric ions. A twofold increase in lipid peroxide in response to paraquat was suppressed significantly by βOHB treatment (Fig. 4E). Thus, βOHB protects against paraquat-induced oxidative stress in mouse kidney.

Our observation that βOHB is an endogenous HDAC inhibitor present in organisms at millimolar concentrations during prolonged fasting and CR reveals an example of integration between metabolic status and epigenetic changes. We show that changes in histone acetylation and gene expression caused by βOHB promote stress resistance in the kidney. Future studies should investigate the specific gene expression and physiological effects of βOHB in other tissues. For example, low-carbohydrate diets that induce substantial ketogenesis are broadly neuroprotective and enhance resistance of neurons to oxidative damage (*20*). In addition, reduction in HDAC activity by either genetic manipulation or chemical inhibition extends life span in *Drosophila* (*21*, *22*). Inhibition of HDACs by βOHB might contribute to the beneficial effect of ketogenic diets and may be one mechanism by which calorie restriction confers health benefits.

References and Notes

1. A. G. Ladurner, *Mol. Cell* **24**, 1 (2006).
2. K. E. Wellen *et al.*, *Science* **324**, 1076 (2009).
3. H. Takahashi, J. M. McCaffery, R. A. Irizarry, J. D. Boeke, *Mol. Cell* **23**, 207 (2006).
4. S. Imai, C. M. Armstrong, M. Kaeberlein, L. Guarente, *Nature* **403**, 795 (2000).
5. E. P. Candido, R. Reeves, J. R. Davie, *Cell* **14**, 105 (1978).
6. G. F. Cahill Jr., *Annu. Rev. Nutr.* **26**, 1 (2006).
7. G. F. Cahill Jr. *et al.*, *J. Clin. Invest.* **45**, 1751 (1966).
8. A. M. Robinson, D. H. Williamson, *Physiol. Rev.* **60**, 143 (1980).
9. L. Laffel, *Diabetes Metab. Res. Rev.* **15**, 412 (1999).
10. J. H. Koeslag, T. D. Noakes, A. W. Sloan, *J. Physiol.* **301**, 79 (1980).
11. B. J. North, B. Schwer, N. Ahuja, B. Marshall, E. Verdin, *Methods* **36**, 338 (2005).
12. O. E. Owen *et al.*, *J. Clin. Invest.* **52**, 2606 (1973).
13. T. Agalioti *et al.*, *Cell* **103**, 667 (2000).
14. C. Van Lint, S. Emiliani, E. Verdin, *Gene Expr.* **5**, 245 (1996).
15. G. J. Kops *et al.*, *Nature* **419**, 316 (2002).
16. K. Kawai *et al.*, *Chem. Res. Toxicol.* **13**, 1275 (2000).
17. S. Nemoto, T. Finkel, *Science* **295**, 2450 (2002).
18. T. Nyström, *EMBO J.* **24**, 1311 (2005).
19. H. Esterbauer, R. J. Schaur, H. Zollner, *Free Radic. Biol. Med.* **11**, 81 (1991).
20. Y. Kim *et al.*, *J. Neurochem.* **101**, 1316 (2007).
21. B. Rogina, S. L. Helfand, S. Frankel, *Science* **298**, 1745 (2002).
22. H. L. Kang, S. Benzer, K. T. Min, *Proc. Natl. Acad. Sci. U.S.A.* **99**, 838 (2002).

Acknowledgments: We thank J. Carroll for graphics, G. Howard and S. Ordway for editorial assistance, V. Fonseca for administrative assistance, and A. Brunet (Stanford University) for reagents. Supported by funds from the Gladstone Institutes.

Supplementary Materials

www.sciencemag.org/cgi/content/full/science.1227166/DC1
Materials and Methods
Figs. S1 to S15
Tables S1 to S3
References (*23*–*26*)

9 July 2012; accepted 16 November 2012
Published online 6 December 2012;
10.1126/science.1227166

Suppression of Oxidative Stress by β-Hydroxybutyrate, an Endogenous Histone Deacetylase Inhibitor

Tadahiro Shimazu *et al.*

Science **339**, 211 (2013);
DOI: 10.1126/science.1227166